

NOISE IDENTIFICATION AND ESTIMATION OF ITS STATISTICAL PARAMETERS BY USING UNSUPERVISED VARIATIONAL CLASSIFICATION

B. Vozel, K. Chehdi, L. Klaine

Vladimir V. Lukin, Sergey K. Abramov

IETR-TSI2M, UMR CNRS 6164
BP 80518, 22305 Lannion Cedex - FRANCE

National Aerospace University,
61070, Kharkov, Ukraine

ABSTRACT

This paper deals with the problem of identifying the nature of the noise and estimating its statistical parameters from the observed image in order to be able to apply the most appropriate processing or analysis algorithm afterwards. We focus our attention on three main classes of degraded images, the first one being degraded by an additive noise, the second one by a multiplicative noise, and the latter by an impulse noise. To improve the identification rate, we propose an unsupervised variational classification through a multi-thresholding method. Each class is then characterized by statistical parameters obtained from homogeneous regions. For the accuracy of the estimation of the noise statistical parameters, we distinguish the corresponding local estimates statistical series according to the number of pixels taken into account to calculate them. The experimental study highlights the improvement so obtained and shows the efficiency and the robustness of the whole method.

1. INTRODUCTION

The majority of filtering algorithms in the literature [10], [8], [9], [5], assume that the nature of the noise and its statistical parameters are known. Whereas in most practical cases, we have no *a priori* knowledge on these data [1], [6]. For this reason, the nature and the statistical parameters of the noise must be estimated as they condition the quality of the filtering or the analysis of the images. In this paper we are interested in the problem of identifying the nature of the noise and then estimating its variance from the observed image. In [4], we prove it is possible to identify the nature of the noise by recording variations of local statistics (the standard deviation as a function of the average) computed in the homogeneous regions of the observed image. If the recording is parallel to the average axis, then the noise is declared as an additive one and its standard deviation is equal to the sampling average of the different values of the local standard deviation. If the recording can be assimilated by a line passing through zero, then the noise is declared as a multiplicative one and its standard deviation is given by the slope of the line. And finally, if the recording can not be viewed as a line passing through zero, then the noise is declared as an impulsive one.

In order to increase the identification rate and to improve the estimation of statistical noise parameters, we propose to use more powerful and advanced refined classification and estimation procedures instead of earlier proposed (old) procedure [4].

Supported by the European Union. Co-financed by the ERDF and the Regional Council of Brittany, through the European Interreg3b PIMHAI project

In section 2, we deal with the detection of homogeneous regions. We first propose an improvement of the classical image multi-thresholding methods. The goal is to achieve the precise determination of homogeneous zones in numerical images by pixels classification. The thresholds and the modes are obtained by minimization of a new energy of gravitational clustering initialized with the significant peaks of a cumulated histogram. Then, the best modes and the best thresholds are calculated by alternate optimization of an energy of multi-thresholding, leading to a piecewise quadratic potential. This energy is built from a total uniformity criterion which measures the homogeneity of a given map of regions. Finally, an unsupervised classification is performed by use of a supervised variational classification approach which minimizes an adapted energy of transitions of phases. The potential which controls the classification process is built from the previously determined best thresholds and modes.

In section 3, we precise the noise identification and estimation of its statistical parameters. Concerning the estimation procedure, the improvement is based on the use of the local statistics calculated by means of the homogeneous regions map obtained in the previous classification stage, while varying the analysis windows size. The analysis of these discrete local estimates statistical series shows that it is not relevant to discriminate them only according to the window size. Indeed, it is better to consider the number of pixels taken into account within the analysis window to calculate them. We thus ensure that two local statistical estimators, belonging to the same set, follow the same statistical law. Then, the expectation of the not-biased local estimates coincides with the noise variance. In practice, we subsequently replace the law expectation by the global empirical mean average on the statistical series. The experimental study is carried out in the last section to show the efficiency and the robustness of the whole method.

2. DETECTION OF HOMOGENEOUS REGIONS

2.1. Motivations

The detection of homogeneous regions by histogram transformation is a difficult task. An histogram can be viewed as multimodal if the modes are sufficiently distant from each other. However, the multi-modality is not well defined as the minimal distance between the modes is not explicitly given. The histogram transformation that we propose, considers an alternative modelling of the histogram by a dynamic representation. The values of the histogram are comparable with the masses and the samples with the positions of a dynamic system of the previously defined masses.

Formally, we allow the histogram to take real values but only in the range of real light intensities I . It must be contained in $C(I)$

the closed convex envelope of I .

The initial vector of the positions \vec{x}^0 is defined by $x_i^0 = i$. The vector of the masses \vec{h} is defined by $\vec{h} = \vec{h}^{\text{cum}}$ where $h_i^{\text{cum}} = \mu^{\text{cum}}(\{i\})$. h_i^{cum} are the significant peaks of the cumulated histogram \vec{h}^{cum} . They are computed from local histograms computed on sliding windows with different sizes (16×16 , 32×32 , 64×64) of the original image. The different sizes of the sliding window allow to take account of the spatial resolution of the image and to get an initial histogram \vec{x}^0 with a well pronounced multi-modal form [7].

2.2. The Gravitational Energy

The energy of gravitational clustering is defined by:

$$Q_{\text{gc}}(\vec{h}; \vec{x}) \triangleq \frac{1}{2} \sum_{i \in I} \sum_{j \in I} h_i h_j \delta_{i,j}(\vec{x}) |x_i - x_j|^2 \quad (1)$$

It measures the dispersion of the positions with regard to the relative centres of gravity. We call *centre of gravity* relative to a position, the barycentre of the positions located within a radius lower than a maximum preset distance and named *gravitational radius*. The gravitational equation is built to cancel the derivative of the energy of gravitational clustering \vec{x} minimize $Q_{\text{gc}}(\vec{h}; \vec{x})$. This equation defines the trajectory of the positions through the gravitational field.

$$\begin{aligned} \vec{x}(0) = \vec{x}^0 \text{ and } \frac{d\vec{x}}{dt}(t) = \vec{G}(\vec{h}; \vec{x}(t)) - \vec{x}(t) \\ t \rightarrow +\infty \end{aligned}$$

Each position can be moved towards its relative centre of gravity. $\vec{x} = \vec{G}(\vec{h}; \vec{x})$ where the gravitational field is given by:

$$\vec{G}(\vec{h}; \vec{x}) \triangleq \mathbf{G}(\vec{h}; \vec{x}) \cdot \vec{x} \quad (2)$$

$$G_{i,j}(\vec{h}; \vec{x}) \triangleq [\sum_{k \in I} \delta_{i,k}(\vec{x}) h_k]^{-1} \delta_{i,j}(\vec{x}) h_j \quad (3)$$

$$\delta_{i,j}(\vec{x}) \triangleq H(R(x_i, x_j) - |x_i - x_j|) \quad (4)$$

The condition $R(x_i, x_j) = \sup(R(x_i), R(x_j)) > |x_i - x_j|$ simply translate the determination of the relative centres of gravity.

The trajectory is simply controlled by the proximity and the importance of specific masses. The positions are attracted by their relative centres of gravity. The gravitational radius is essential to precisely quantify the multi-modality with regard to the positions of the modes.

Thus, the gravitational clustering returns a vector of the positions gradually constant on each class. Visually, the vector of the positions takes a staircase shape. The positions are converted into integer values to preserve a meaning in the set of light intensities. The histogram corresponding to \vec{x}^∞ is denoted histogram of the centres of gravity $h^{\text{gc}}(\cdot)$. It is multimodal and the modes are given by the various levels of the vector \vec{x}^∞ .

2.3. The Multi-Thresholding Energy Criterion

The thresholds and the modes must be ordered so that each mode lies between two consecutive thresholds. The aim of this section is to determine the best thresholds and the best modes with regard to a criterion denoted *the total uniformity criterion*. This choice is not coarse and the most intuitive is not necessarily the best.

The *total uniformity criterion* measures the quality of a map of homogeneous regions. Its principle is built on the idea that an area is *uniform* if the dispersion of the grey levels is weak.

We can measure the uniformity of an area by estimating the *intra-area variance*. We estimate the *total uniformity* of a map by the weighted average, by the size of the different regions, of the intra-area variances. The energy of multi-thresholding is built in order to coincide exactly with the total uniformity if the modes are equal to the intra-area means. It measures the quality of the modes and the thresholds knowing their number. This quality is estimated by regarding the vector of the thresholds as an approximation in N samples of the histogram. Its discrete version is given by:

$$\begin{aligned} Q_{\text{mt}}(h; \vec{s}, \vec{m}) \triangleq \frac{1}{2} \sum_{k=0}^N \sum_{x_j < s_{k+1}} \sum_{x_j > s_k} h_j |x_j - m_k|^2 \\ + \frac{1}{2} \sum_{k=1}^{N-1} \sum_{x_j = s_k} h_j \min(|x_j - m_k|^2, |x_j - m_{k+1}|^2) \end{aligned} \quad (5)$$

The optimal solution consists of a continuation which alternatively minimizes the multi-thresholding energy with regard to the modes and the thresholds. Assuming the modes \vec{m} known, the energy of multi-thresholding $Q_{\text{mt}}(h; \vec{s}, \cdot)$ is convex with respect to the thresholds. It admits a single minimum. This one is simply given by the middle of the interval ranging between two modes:

$$s_k^n = (m_k^n + m_{k+1}^n) / 2 \quad (6)$$

Assuming the thresholds \vec{s} known, the vector of the modes which minimizes the multi-thresholding energy is given by the barycentres of the thresholds whose weights depend on the thresholds and the histogram:

$$m_k^{n+1} = M_k(h; \vec{s}^n) \quad (7)$$

2.4. Unsupervised Variational Classification

When the image is seriously degraded, the *a priori* homogeneity constraint can be introduced by adding to the usual classification term, defined by a potential, an additional regularization term translating the homogeneity constraint [11], [3, 2]. In our work, this classification method becomes attractively unsupervised since the potential is automatically given from the best thresholds \vec{s}^{mt} and the best modes \vec{m}^{mt} obtained at convergence. It is sufficient for that to build a potential whose stable phases are given by the modes. The unstable phases are then given by the thresholds. Given $(\vec{s}, \vec{m}) \in \mathbb{R}^{2N+1}$ a couple of thresholds and modes, the image u , then we define the potential $W(\vec{s}, \vec{m}; \cdot) : \mathbb{R} \mapsto \mathbb{R}^+$ by:

$$\begin{aligned} W(\vec{s}, \vec{m}; u) \triangleq \begin{cases} +|u - m_1|^2 / |m_1 - s_1|^2 & \text{if } u \in] -\infty, s_1 - \eta[, \\ +|u - m_k|^2 / |m_k - s_{k-1}|^2 & \text{if } u \in]s_{k-1} + \eta, m_k - \eta[, \\ -|u - s_k|^2 / |s_k - m_k|^2 + A_k(\eta) & \text{if } u \in]s_k - \eta, s_k + \eta[, \\ +|u - m_k|^2 / |s_k - m_k|^2 & \text{if } u \in]m_k + \eta, s_k - \eta[, \\ +|u - m_N|^2 / |m_N - s_{N-1}|^2 & \text{if } u \in]s_{N-1} + \eta, +\infty[. \end{cases} \quad (8) \end{aligned}$$

with $A_k(\eta) \triangleq 1 - 2\eta / |s_k - m_k| + 2\eta^2 / |s_k - m_k|^2$ to get a sufficiently regular potential. In practice, the value of η is taken very near or equal to zero. Then, Q_{pt} writes:

$$Q_{\text{pt}}(W, \varphi, \varepsilon; u) \triangleq \int_{\Omega} \left[\varepsilon \varphi(|\nabla u|) + \frac{1}{\varepsilon} W(u) \right] \quad (9)$$

Two different schemes can be considered to get the solution. The first scheme, denoted [Sams¹] in the experimental study, realizes a direct minimization of the dynamic equation associated with (9) [11] and [3, 2]. A second scheme, denoted [Sams²], performs an alternate minimization using the semi-quadratic algorithm [11] and [3, 2].

3. NOISE IDENTIFICATION AND ESTIMATION

In order to identify the nature of the noise, we need to calculate local estimates of its statistical parameters. To calculate the local statistics of interest $\text{mean}_{\Phi(u)_{i,j}}$, $(\text{var}_{\Phi(u)_{i,j}}^*)$, we make use of the homogeneous regions map u_h^{lab} , obtained at the output of the previous classification stage. We consider analysis windows with different increasing size. We chose the following local estimation kernel $\Phi_{[V]}^{lab}(v)$. This kernel takes into account all the pixels within the greatest under-area of the neighborhood $(i, j) + [V]$:

$$\Phi_{i,j,i',j'} \triangleq \begin{cases} 1 & \text{if } (u_h^{lab})_{i',j'} \text{ is the most frequent label,} \\ 0 & \text{otherwise,} \\ & (i', j') \in (i, j) + [V] \end{cases} \quad (10)$$

where u_h is a map of homogeneous regions and $[V]$ the analysis sub-window. The initial method was based on the discrimination of the statistical series according to the window size. The analysis of the corresponding discrete local statistical series shows that it is not relevant to discriminate them only according to the window size. Indeed, it is better to consider the number of pixels taken into account. We thus ensure that two local statistical estimators, belonging to the same set and then calculated with the same number of pixels, follow the same statistical law. It should be noted that this law is *a priori* unknown, except for the Gaussian additive noise variance. In this last case, it is a χ^2 law. For each number of pixels taken into account, we obtain a coherent list of statistics.

Identification of the nature of the noise: We now consider that the most representative list is that which contains the most elements at the output of the preceding classification procedure of local statistical estimators. We fit a polynomial regression to the set of variance estimates, according to the average estimates $\text{mean}_{\Phi(u)_{i,j}}$. We decide the noise is additive if the zero order polynomial regression gives the best approximation within the meaning of least squares criterion. The noise is multiplicative if the best approximation is obtained by the second order regression.

Estimate of the variance of the noise: The initial method [4] considers the most frequent standard deviation estimate from the global histogram of the corresponding statistical series $(\text{var}_{\Phi(u)_{i,j}}^*)$ and without discriminating them according to the number of pixels involved in their calculation. It is better, on one hand to re-use the newly discriminated statistical series obtained in the preliminary identification phase, and on the other hand, to calculate the estimators expectation. Indeed, the expectation of the not-biased local variance estimates $E[\text{var}_{\Phi(u)_{i,j}}^*]$ coincides with the additive noise variance. In the same way, the expectation of the ratio of the not-biased local variance on the square of the local mean average coincides with the multiplicative noise variance. The necessary condition is that all the estimators must follow the same statistical law. This is satisfied if we consider statistical series indexation by the number of pixels taken into account to calculate local estimates. In practice, we replace the law expectation by the global empirical mean average on the statistical series. The noise variance is jointly estimated to the identification process, since the

noise variance estimates are related to the polynomial regression coefficients. However from a theoretical point of view, it is necessary to also take account of the pixels spatial proximity. Indeed, estimates calculated on connected neighborhoods are probably not independent.

4. EXPERIMENTAL RESULTS

We present afterwards the original image [SAVOISE] of the french data bank of the GDR-CNRS, the degraded image, the potential $W(\vec{s}, \vec{m}; \cdot)$ used to control the classification, as well as the obtained map of homogeneous regions (Fig.1). In order to objectively evaluate the classification results, we also estimate the total uniformity measure on the original images using each obtained map of homogeneous regions.

The method of classification using the alternate minimization [Sams²] is better provided that the parameter of regularization is well selected. However, it is much slower and more constraining than the method using direct minimization [Sams¹]. The results obtained by the latter are quite good and easier to control.

The procedure of noise identification was tested on various images [BOAT], [BUREAU], [CAMERA], [CORNOUAILLE], [COULOIR], [FEMME], [LENA], [VOITURE], [SAVOISE] and [TEXTURE]. Different noise levels were considered for the additive noise hypothesis $\sigma_b = 10, 12, 14$, for the multiplicative noise hypothesis $\sigma_n = 0.1, 0.2, 0.3$, as well as different values of the probability $p = 0.2, 0.3, 0.4$ of the Bernoulli density probability function of the impulse noise. We generated a set of thirty images degraded by an additive noise, thirty images degraded by a multiplicative noise and thirty images degraded by an impulse noise. The result of the proposed identification method was compared to the results of the previously developed identification method. The procedure of identification of the additive or multiplicative noise benefits from the rigorous classification of the local statistics and the use of a least squares method to the second order 2 on the variance estimates rather than applying a first order regression method on the standard deviation estimates (tab. 1).

The procedure of noise variance estimation was tested also on the image [SAVOISE]. This image presents the advantage of being in its original version almost a map of regions. That enables us to use it like a ground truth map. We chose to degrade this image by first additive noise with different standard deviation levels $\sigma_b = 10, 12, 14$, and then multiplicative noise with also different standard deviation levels $\sigma_n = 0.1, 0.2, 0.3$. In order to test the robustness of the proposed system, we carried out tests by taking as map of regions: the original image [truth], the results of the initial multi-thresholding method [7], denoted hereafter [Kerm], the results of the classification method by direct minimization [Sams¹] and then by alternate minimization [Sams²], all three last methods applied on the image degraded by an additive noise $\sigma_b = 14$ (tab. 2).

The new approaches provide overall better results. Not so good quality of the homogeneous regions map leads to worse results [Kerm]. It translates the sensitivity of the proposed method to the quality of the preliminary homogeneous regions map. Good quality of the homogeneous regions map allows us to get quasi-perfect results [Sams²]. More, this also confirms the interest to develop homogeneous zones detection methods robust to the noise level. We should recall here that the noise variance is estimated simultaneously to the additive or multiplicative noise identification process. It is possible to show in experiments that the noise vari-

	Detected as					
	Additive		Multiplicative		Impulse	
	Old	New	Old	New	Old	New
additive	28	29	2	1	0	0
multiplicative	3	3	25	25	2	2
impulse	1	0	0	0	29	30

Table 1. Comparative results of the two noise identification procedures - Old:[4] - New:proposed

		Additive			Multiplicative		
		10	12	14	0.1	0.2	0.3
		[Truth]	Old	9.733	11.733	13.733	0.098
	New	10.037	12.040	14.044	0.100	0.201	0.301
[Kerm]	Old	5.315	6.184	6.344	0.048	0.183	0.290
	New	5.652	6.699	7.768	0.056	0.190	0.295
[Sams ¹]	Old	9.165	11.251	12.961	0.094	0.180	0.289
	New	9.580	11.486	13.395	0.096	0.200	0.300
[Sams ²]	Old	9.959	11.690	14.234	0.098	0.193	0.285
	New	10.080	12.067	14.060	0.101	0.202	0.302

Table 2. Comparative results of the four noise variance estimation procedures on the image [SAVOISE]

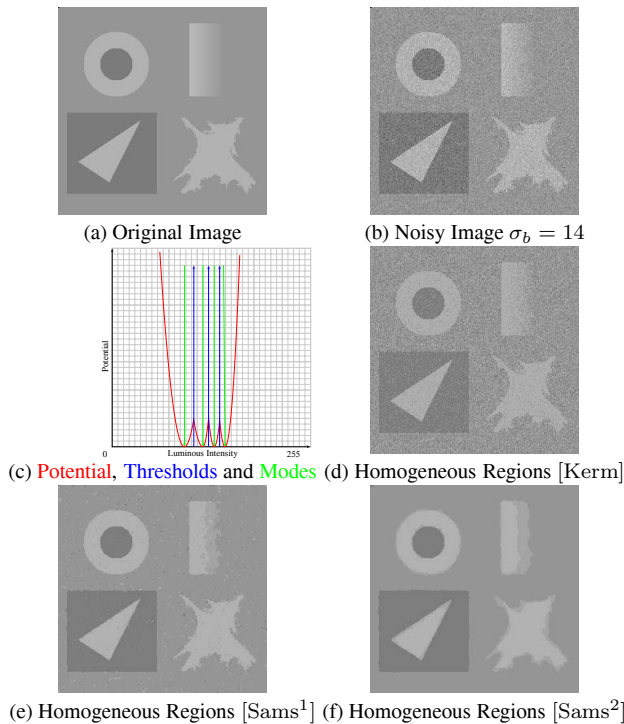


Fig. 1. Detection of Homogeneous Areas on image [SAVOISE] degraded by an additive noise $\sigma_b = 14$

ance estimate stabilizes iterations. In other words, the assumption of the a priori knowledge of the noise variance in the procedure of homogeneous zones detection is not a drawback.

The use of classified local statistics on regions detected as homogeneous together with the corresponding homogeneous regions map leads to a rather significant improvement in comparison to the previously developed (old) method. The most important contributions come from a better accurate homogeneous map and a refined consistent use of local statistics. They lead in particular to better robustness of the proposed joint procedure of noise identification and estimation. Better precision of the results can be highlighted. We can notice also the new scheme is faster and less resource-consuming since the local statistics are never stored.

5. SUMMARY AND CONCLUSIONS

Classification of degraded images with different noise levels show the potential of the whole system: it is rather effective for the determination of homogeneous regions in an image, and allows a significant improvement of noise identification and estimation. The proposed method has the main advantage to be optimal and robust to the observation noise.

6. REFERENCES

- [1] L. Alparone, F. Argenti, and G. Torricelli. Modelling and assessment of signal-dependent noise for image de-noising. In *Proceedings of EUSIPCO'02, Toulouse*, pages 287–290, 2002.
- [2] G. Aubert, L. Blanc-Féraud, and R. March. Γ -convergence of discrete functionals with non-convex perturbation for image classification. Technical Report 4560, Institut National de Recherche en Informatique et en Automatique, September 2002.
- [3] G. Aubert and P. Kornprobst. *Mathematical problems in image processing (Partial differential equations and the calculus of variations)*. Springer, 2002.
- [4] L. Beaupaire, K. Chehdi, and B. Vozel. Identification of the nature of noise and estimation of its statistical parameters by analysis of local histograms. In *Proceedings of ICASSP'97, April 21-24, Munich*, 1997.
- [5] A. Buades, B. Coll, and J.-M. Morel. Image denoising by non-local averaging. In *Proceedings of ICASSP'05, Philadelphia, (II)*, pages 25–28, 2005.
- [6] M.P. Carton-Vandecandelaere, B. Vozel, L. Klaine, and K. Chehdi. Application to multispectral images of a blind identification system for blur, additive, multiplicative and impulse noises. In *Proceedings of EUSIPCO'02, Toulouse*, pages 283–286, 2002.
- [7] C. Kermad and K. Chehdi. Research of an automatic and unsupervised system of segmentation. *Image and Vision Computing, Edition Elsevier*, pages 541–555, 2002.
- [8] A. Kurekin, V. Lukin, A. Zelensky, P. Koivisto, and J. Astola. Comparison of component and vector filter performance with application to multichannel and color image processing. In *Proc. of the IEEE-EURASIP Workshop on Nonlinear Signal and Image Processing, Antalya, Turkey*, pages 38–42, 1999.
- [9] T. Lee and X.-L. Meng. A self-consistent wavelet method for denoising images with missing pixels. In *Proceedings of ICASSP'05, Philadelphia, II*, pages 41–44, 2005.
- [10] L. Rudin and S. Osher. Nonlinear total variation based noise removal algorithms. In *Physica D (60)*, pages 259–268, 1992.
- [11] C. Samson, L. Blanc-Féraud, G. Aubert, and J. Zerubia. A variational model for image classification and restoration. *IEEE Transaction on Pattern Analysis and Machine Intelligence*, 22(5):460–472, May 2000.